ACES Asian Chemical Editorial Society

DOI: 10.1002/asia.201800191

CHEMISTRY AN ASIAN JOURNAL Communication

Bimetallic Nanocrystals

Control of the Interfacial Wettability to Synthesize Highly Dispersed PtPd Nanocrystals for Efficient Oxygen Reduction Reaction

Hao Wei[+],[a] Zhi-Yi Hu[+],[a, c] Yu-Xuan Xiao,[a] Ge Tian,[a] Jie Ying,*[a, b] Gustaaf Van Tendeloo,[c, d] Christoph Janiak,[e] Xiao-Yu Yang,*[a] and Bao-Lian Su[a, f]

Abstract: Highly dispersed PtPd bimetallic nanocrystals with enhanced catalytic activity and stability were prepared by adjusting the interfacial wettability of the reaction solution on a commercial carbon support. This approach holds great promise for the development of high-performance and low-cost catalysts for practical applications.

The proton exchange membrane fuel cell (PEMFC) is one of the most promising clean energy conversion techniques due to its high power density, low working temperature, and zero pollutant emission.[1] The widespread commercialization of PEMFC is impeded by the sluggish kinetics of the oxygen reduction reaction (ORR) at the cathode.[2] Pt-based nanomaterials are currently the most efficient catalysts in ORR.[3] However, the low abundance and high cost of Pt as well as the poor stability greatly limit their practical applications.[4] A universal strategy for enhancing both catalytic performance and utilization efficiency of Pt is to utilize Pt-based alloys instead of pure Pt as the catalysts due to the favorable synergistic effect between each metal.[5]

Moreover, exploitation of support materials has been extensively studied to improve the catalytic activity and stability of catalysts.[6] The loss of surface active sites due to aggregation and/or Ostwald ripening is the major issue that results in the fast degradation of supported catalysts.[7] To overcome this problem, substitute efforts have been devoted to preparation of highly dispersed catalysts on supports, which could efficiently prevent the occurrence of aggregation and/or Ostwald ripening due to the confinement effect of matrix materials.[8] Many successful methods, such as ion exchange/wetness impregnation,[9] in situ encapsulation,[10] organic modification,[11] and nanoencapsulation,[12] had been developed for preparing catalysts with high dispersion. With increasing requirements for highly dispersed nanometals in practical applications, further progress has been achieved. For example, a photochemical deposition method was reported by Xia's group to synthesize highly dispersed Pt nanoparticles on porous nanofibers.[13] A high-viscosity-solvent method was presented by our group to prepare PtPd nanocrystals highly dispersed in various *meso*-materials.[14] Despite these notable achievements, two major disadvantages have to be pointed out: i) those reported synthetic procedures are usually complex and/or need harsh conditions, which are not suitable for upscaling in commercialization; ii) the fabrication of supported materials is generally cumbersome and time-consuming that means their cost is expensive. Therefore, a procedure to prepare highly dispersed Pt-alloy catalysts that can effectively solve the aforementioned issues is highly desired for industrial applications.

The wettability is a very important property of material surfaces/interfaces, and can be altered by adjusting the chemical composition and surface microstructure.[15] Highly dispersed nanometals could also be prepared by utilizing this property, such as surface functionalization and hydrophobicity control of support materials.[16] However, the control of wettability of support materials during the synthesis procedure of metal nano-

[a] *H. Wei,[+] Dr. Z.-Y. Hu,[+] Y.-X. Xiao, Dr. G. Tian, Dr. J. Ying, Prof. X.-Y. Yang, Prof. B.-L. Su*
State Key Laboratory Advanced Technology for Materials Synthesis and Processing, School of Materials Science and Engineering
Wuhan University of Technology
122, Luoshi Road, Wuhan (China)
E-mail: whutyingjie@gmail.com
xyyang@whut.edu.cn

[b] *Dr. J. Ying*
Department of Chemical Engineering
University of Waterloo
Ontario, N2L 3G1 (Canada)

[c] *Dr. Z.-Y. Hu,[+] Prof. G. Van Tendeloo*
NRC (Nanostructure Research Centre)
Wuhan University of Technology
122, Luoshi Road, Wuhan (China)

[d] *Prof. G. Van Tendeloo*
EMAT (Electron Microscopy for Materials Science)
University of Antwerp
Groenenborgerlaan 171, 2020 Antwerpen (Belgium)

[e] *Prof. C. Janiak*
Institut für Anorganische Chemie und Strukturchemie
Heinrich-Heine-Universität Düsseldorf
40204 Düsseldorf (Germany)

[f] *Prof. B.-L. Su*
Laboratory of Inorganic Materials Chemistry (CMI)
University of Namur
61 rue de Bruxelles, 5000 Namur
(Belgium)

[+] *These authors contributed equally to this work.*

Supporting information and the ORCID identification number(s) for the author(s) of this article can be found under https://doi.org/10.1002/asia.201800191.

materials in an effort to synthesize nanometals with high dispersion is quite rare. Herein, we present a facile interfacial wettability method to prepare highly dispersed PtPd bimetallic nanoparticles on Vulcan carbon (XC-72) by controlling the hydrophilic/hydrophobic relationship between reaction solvent and support. The rationale for choosing Vulcan carbon as the support is due to its mature production technology and low price as a commercial product, and good conductivity and high surface area as a common electrocatalyst support. Notably, when using hydrophobic Vulcan carbon as the support material in the hydrophilic reaction solution of 1,5-pentanediol during the metal synthesis, PtPd nanoparticles with high dispersion (denoted as PtPd/C) were obtained. While using hydrophilic oxidized Vulcan carbon as the support under the same synthesis conditions, aggregated PtPd nanoparticles (denoted as PtPd/OC) were formed. Compared to both PtPd/OC and commercial Pt/C catalysts, the PtPd/C sample exhibits superior electrocatalytic activity and durability in ORR.

The PtPd/C sample was prepared by using a hydrothermal synthesis method in 1,5-pentandiol solution (act as the solvent and the reducing agent) with polyvinylpyrrolidone (PVP) as the surfactant in the presence of Vulcan carbon (see the Supporting Information for the experimental details). These as-synthesized products were initially examined by powder X-ray diffraction (PXRD). As shown in Figure S1, the broad peak at about 25° represents the existence of amorphous carbon and the other three peaks at 40.0°, 46.6°, and 68.0° can be readily indexed to the (111), (200), and (220) reflections of face-centered cubic (fcc) PtPd. These three peaks are slightly shifted to lower 2 theta values in comparison with the corresponding peaks of Pd crystal, indicating that the Pt atoms had been inserted into the lattice of Pd crystal and caused the increase of lattice parameters.[15] In particular, these three peaks for PtPd crystals are broadened, demonstrating their nanoscale structural features.

Representative electron microscopy images of the as-synthesized PtPd/C sample are shown in Figure 1. High angle annular dark field scanning transmission electron microscopy (HAADF-STEM) image (Figure 1 A) shows that a large number of nanoparticles with an average size of about 5 nm are highly dispersed on the surface of carbon spheres. High resolution TEM (HRTEM) image (Figure 1 B) clearly shows that these nanoparticles exhibit well-defined lattice fringes, indicating their good crystallinity. The fast Fourier transformation (FFT) of PtPd/C (inset of Figure 1 B) shows both concentric rings and discrete diffraction spots, indicating that these PtPd nanoparticles are highly crystalline with a fcc polycrystalline structure. To characterize the elemental distribution in these nanoparticles, PtPd/C sample was measured by HAADF-STEM energy-dispersive X-ray spectroscopy (HAADF-STEM-EDX). As shown in Figure 1 C–F, Pt elements are distributed on the surface of nanoparticles while Pd elements are only located in the center of nanoparticles, displaying a typical core-shell nanostructure with a Pt surface layer.

X-ray photoelectron spectroscopy (XPS) was used to investigate the surface composition of the PtPd/C sample. The surveyed spectra (Figure S2A) demonstrated that there are Pt, Pd, C, and O elements in the sample. The high resolution Pt 4f and Pd 3d spectra were deconvoluted. For Pt 4f line (Figure S2B), the principle peaks were attributed to Pt° at 71.4 eV ($4f_{7/2}$) and 74.7 eV ($4f_{5/2}$), while the peaks at 72.8 eV ($4f_{7/2}$) and 76.1 eV ($4f_{5/2}$) were assigned to Pt in the 2+ oxidation state.[16] For Pd 3d line (Figure S2C), the principle peaks at 334.5 eV ($3d_{5/2}$) and 339.8 eV ($3d_{3/2}$) represented for Pd° and peaks at 335.2 eV ($3d_{5/2}$) and 340.8 eV ($3d_{3/2}$) stood for Pd^{2+}.[17] The deconvolution results of the Pt 4f and Pd 3d spectra also suggests that ▫ 73% surface Pt and ▫ 72% surface Pd are in the metallic state while ▫ 27% surface Pt and ▫ 28% surface Pd are in the oxidized state.

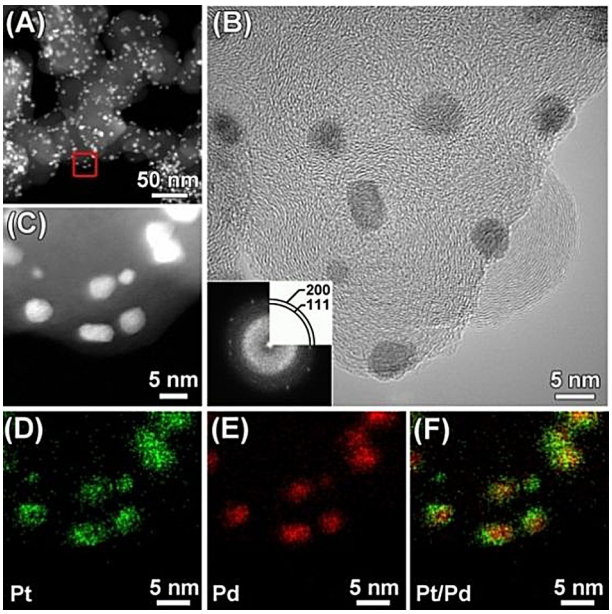

Figure 1. (A) HAADF-STEM image of PtPd/C at low magnification. (B) HRTEM image of PtPd/C and corresponding FFT of the whole area (inset). (C) HAADF-STEM image of PtPd/C at high magnification of the area indicated by red box in (A), and (D-F) corresponding EDX elemental maps: Pt (green) and Pd (red).

To better understand the formation mechanism of highly dispersed PtPd nanoparticles in our synthesis, the effect of hydrophilic/hydrophobic property of the support materials in the reaction system was investigated in detail. Vulcan carbon, similar to carbon simple substance, is naturally hydrophobic due to the low molecular polarity of carbon.[18] The contact angle test shows that Vulcan carbon has a high contact angle of 135° with water (Figure S3A), indicating its hydrophobic feature. To change the hydrophilic/hydrophobic property, Vulcan carbon was oxidized by acid treatment (see the Supporting Information for details). After oxidation, the Vulcan carbon turned to be hydrophilic, which was proven by the contact angle test (Figure S3B) due to the introduction of the hydrophilic groups of hydroxyl and carboxyl (Figure S4 and the accompanying text). Then, PtPd/OC sample was prepared under the same conditions used in the synthesis of PtPd/C sample but replacing Vulcan carbon with oxidized Vulcan carbon. Figure 2 shows the proposed formation mechanism of PtPd nanoparticles on a hydrophobic support (Vulcan carbon; Fig-

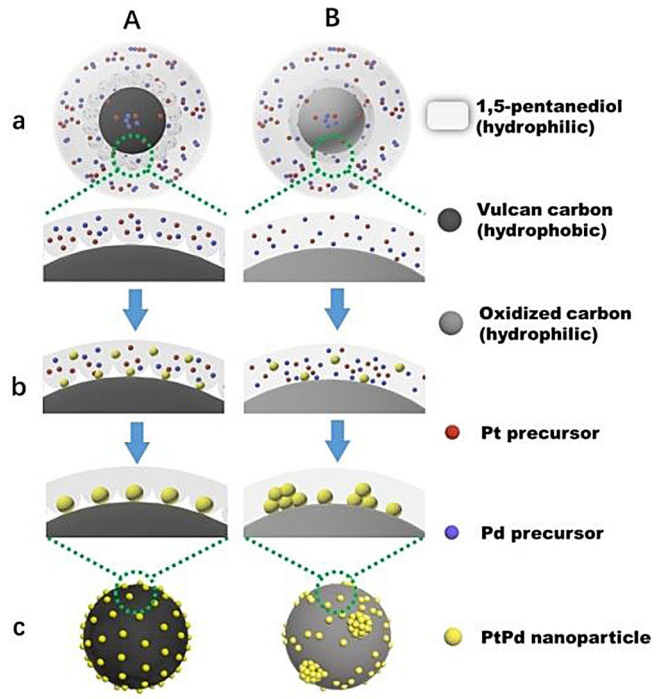

Figure 2. Schematic illustration of the proposed formation mechanism of PtPd nanocrystals prepared in the presence of (A) hydrophobic Vulcan carbon and (B) hydrophilic oxidized Vulcan carbon: (Aa and Ba) dispersing of metal precursors and support materials in reaction solution; (Ab and Bb) reducing metal precursors after thermal treatment; (Ac and Bc) producing the supported metal nanocrystals.

ure 2A) and a hydrophilic support (oxidized Vulcan carbon; Figure 2B). In the synthesis, the metal precursors and support materials are firstly dispersed in the solvent of 1,5-pentandiol. Due to the inverse correlation between hydrophilic solvent and hydrophobic Vulcan carbon, the reaction solution has poor wettability on the surface of Vulcan carbon, which means the contact area between the reaction solution and Vulcan carbon is relatively small (Figure 2Aa). During the metal nucleation and growth stage, the deposition speed of the primary synthesized nanoclusters/nanoparticles on the support can be consequently slowed down (Figure 2Ab), which can effectively avoid the metal aggregation. Additionally, the small contact area can also prevent the anchored nanoclusters/nanoparticles to overgrow. Thus, PtPd nanoparticles with small size and high dispersion are obtained (Figure 2Ac). In contrast, because of the same hydrophilic properties of both the reaction solution and support materials, their contact area is much bigger (Figure 2Ba). So the primary synthesized nanoclusters/nanoparticles could be deposited on the support fast and easy to overgrow (Figure 2Bb), resulting in the aggregation and large size of the as-synthesized PtPd nanoparticles (Figure 2Bc). TEM results confirm the above-mentioned difference of obtained PtPd nanoparticles synthesized in the hydrophobic support (Figure 1A and Figure S5) and the hydrophilic support (Figure S6) under otherwise same synthesis conditions. Therefore, our results demonstrate that highly dispersed metal nanoparticles can be simply and efficiently synthesized by controlling the hydrophilic/hydrophobic relationship between reaction solvent and support.

The electrocatalytic properties of PtPd/C sample toward the ORR were evaluated. For comparison, PtPd/OC and commercial Pt/C (20 wt% Pt, JM) catalysts were also measured. Figure 3A shows the cyclic voltammetry (CV) curves of these three catalysts performed in N_2-purged 0.1 m $HClO_4$ solutions at room temperature with a sweep rate of 50 mV s^{-1}. The electrochemically active surface area (ECSA) was estimated by integrating the charge collected in the hydrogen adsorption/desorption region (0.05–0.35 V) after double-layer correction, assuming that the value of the adsorption of a hydrogen monolayer is 0.21 mC cm^{-2}. The obtained value of the ECSA based on Pt mass for PtPd/C sample is 74.6 m^2 g^{-1}, which is much higher than that of PtPd/OC sample (38.7 m^2 g^{-1}), and slightly higher than that of the commercial Pt/C catalyst (71.0 m^2 g^{-1}). The

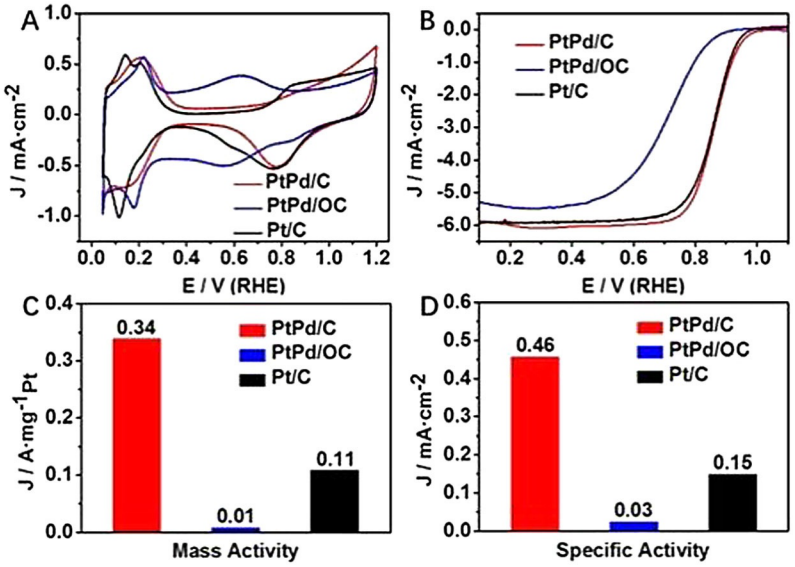

Figure 3. (A) CV curves, (B) ORR polarization curves (C) mass activity and (D) specific activity of PtPd/C, PtPd/OC, and commercial Pt/C catalysts.

ORR measurements were performed on a glassy carbon rotating disk electrode (RDE) at room temperature in O_2-saturated 0.1 m $HClO_4$ solutions at a sweep rate of 10 mV s^{-1}. Figure 3B shows the ORR polarization curves of PtPd/C, PtPd/OC, and commercial Pt/C catalysts. The kinetic current density was calculated based on the Koutecky–Levich equation[19] and then normalized with respect to the loading amount of Pt and ECSA to obtain the mass activity and specific activity, respectively (Table S1). As shown in Figure 3C, the PtPd/C sample displays a mass activity of 0.34 A mg_{Pt}^{-1} at 0.9 V vs. a reversible hydrogen electrode (RHE), which is 34 and 3 times greater than that of the PtPd/OC sample (0.01 A mg_{Pt}^{-1}) and the commercial Pt/C catalyst (0.11 A mg_{Pt}^{-1}), respectively. Similar trends can also been found in the specific activities of these catalysts (Figure 3D). The specific activity of PtPd/C sample (0.46 mA cm^{-2}) is 15 and 3 times greater than that of the PtPd/OC sample (0.03 mA cm^{-2}) and the commercial Pt/C catalyst (0.15 mA cm^{-2}). The Tafel plots can also demonstrate the superior mass activity and specific activity of PtPd/C sample (Figure S7), which are better than that of the previously reported PtPd/C catalysts (Table S2). The superior ORR activity of the PtPd/C sample can be reasonably attributed to their bimetallic composition, high dispersion on carbon support and fast electron transfer (Figure S8 and the companying text).

Since the durability of catalysts is regarded as one of the most important challenges that hinder the commercialization of PEMFCs, we also evaluated the long-term electrochemical stability of PtPd/C and commercial Pt/C catalysts by using accelerated durability tests (ADTs). The ADTs were conducted by applying a cyclic potential between 0.6 and 1.1 V vs. RHE in O_2-saturated 0.1 m $HClO_4$ at room temperature with a scan rate of 50 mV s^{-1}. Figure 4A,B show the CV curve changes of the PtPd/C sample and the commercial Pt/C catalyst at different cycles during ADTs. With increasing numbers of CV cycles, the PtPd/C sample exhibits a slight drop for the currents of the peaks in the hydrogen adsorption/desorption potential regions between 0.05–0.35 V vs. RHE (Figure 4A). By comparison, the currents of the peaks in the same potential regions for the commercial Pt/C catalyst display a significant drop (Figure 4B). The values of normalized ECSA of the PtPd/C sample and the commercial Pt/C catalyst at different cycles are shown in Figure 4C. After 3000 potential cycles, the PtPd/C sample displays only 30% loss in their ECSA, while the ECSA of the commercial Pt/C catalyst shows a significant loss of 62%, demonstrating that the durability of the PtPd/C sample is much better than that of the commercial Pt/C catalyst. To reveal the reasons for their different durability behaviours, the morphologies of these catalysts after durability tests were also measured by TEM. As shown in Figure 4D, the PtPd/C sample shows no obvious change in terms of particle size and dispersity after ADT. In contrast, serious aggregation and sintering happened to the commercial Pt/C catalyst (Figure S9), leading to the significant decrease of their ECSA. Overall, in comparison with the commercial Pt/C catalyst, the PtPd/C sample with high dispersion and bimetallic structure demonstrates a greatly enhanced activity, stability, and durability toward ORR. Considering their synthesis features, such as facile and low-cost, the as-synthesized PtPd/C sample is highly expected to promote the development of next-generation high-performance PEMFC catalysts.

In conclusion, we have proposed an efficient interfacial wettability method to prepare highly dispersed PtPd bimetallic nanoparticles by adjusting the hydrophilic/hydrophobic properties of support materials. The formation mechanism of highly dispersed PtPd nanoparticles has been illustrated. The as-synthesized PtPd/C sample is highly active and durable in the ORR, benefiting from their high dispersion and bimetallic composition. This efficient method is favorable for the facile synthesis of highly dispersed catalysts with excellent performance in various applications.

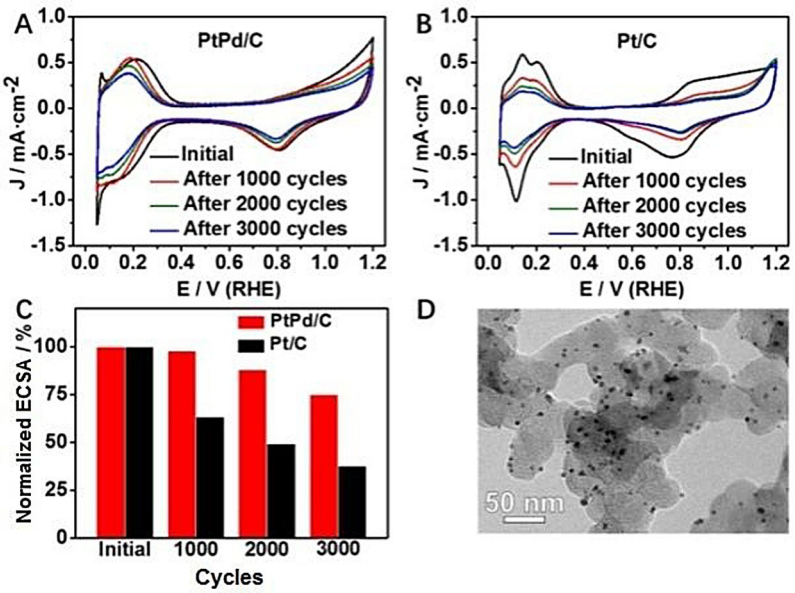

Figure 4. CV curves for (A) PtPd/C and (B) commercial Pt/C catalysts before and after various numbers of cycles. (C) Normalized ECSA calculated by ADT results and (D) TEM image of PtPd/C after 3000 cycles of ADT.

Acknowledgements

This work supported by National Key R&D Program of China (2017YFC1103800), PCSIRT (IRT 15R52), NSFC (U1663225, U1662134, 51472190, 51611530672, 21711530705, 51503166), ISTCP (2015DFE52870), HPNSF (2016CFA033, 2017CFB487), and Open Project Program of State Key Laboratory of Petroleum Pollution Control (Grant No. PPC2016007), CNPC Research Institute of Safety and Environmental Technology, SKLPPC.

Conflict of interest

The authors declare no conflict of interest.

Keywords: high dispersion · oxygen reduction reaction · palladium · platinum · wettability

[1] a) C. R. Raj, A. Samanta, S. H. Noh, S. Mondal, T. Okajima, T. Ohsaka, *J. Mater. Chem. A* **2016**, *4*, 11156 – 11178; b) M. E. Scofield, H.-Q. Liu, S. S. Wong, *Chem. Soc. Rev.* **2015**, *44*, 5836 – 5860; c) M. Zhou, H.-L. Wang, S.-J. Guo, *Chem. Soc. Rev.* **2016**, *45*, 1273 – 1307.

[2] a) B. Kang, J. Y. Lee, *J. Phys. Chem. C* **2014**, *118*, 12035 – 12040; b) F. Wang, P. Wei, G. Yu, J. Liu, *Chem. Eur. J.* **2016**, *22*, 382 – 389; c) J. An, B. Kim, I. S. Chang, H. S. Lee, *J. Power Sources* **2015**, *278*, 534 – 539.

[3] a) X. Zhou, Y. Gan, J. Du, D. Tian, R. Zhang, C. Yang, Z. Dai, *J. Power Sources* **2013**, *232*, 310 – 322; b) S. Guo, S. Zhang, S. Sun, *Angew. Chem. Int. Ed.* **2013**, *52*, 8526 – 8544; *Angew. Chem.* **2013**, *125*, 8686 – 8705; c) H. Huang, K. Li, Z. Chen, L. Luo, Y. Gu, D. Zhang, C. Ma, R. Si, J. Yang, Z. Peng, J. Zeng, *J. Am. Chem. Soc.* **2017**, *139*, 8152 – 8159.

[4] a) Y. Shao, G. Yin, Y. Gao, *J. Power Sources* **2007**, *171*, 558 – 566; b) Y. Nie, L. Li, Z. Wei, *Chem. Soc. Rev.* **2015**, *44*, 2168 – 2201; c) Y. Xu, B. Zhang, *Chem. Soc. Rev.* **2014**, *43*, 2439 – 2450; d) Z. Yang, Z. Yao, G. Li, G. Fang, H. Nie, Z. Liu, X. Zhou, X. Chen, S. Huang, *ACS Nano* **2012**, *6*, 205 – 211; e) M. Li, Z. Zhao, T. Cheng, A. Fortunelli, C. Chen, R. Yu, Q. Zhang, L. Gu, B. V. Merinov, Z. Lin, E. Zhu, T. Yu, Q. Jia, J. Guo, L. Zhang, W. A. Goddard III, Y. Huang, X. Duan, *Science* **2016**, *354*, 1414 – 1419.

[5] a) X. Huang, Z. Zhao, L. Cao, Y. Chen, E. Zhu, Z. Lin, M. Li, A. Yan, A. Zettl, Y. M. Wang, X. Duan, T. Mueller, Y. Huang, *Science* **2015**, *348*, 1230 – 1234; b) V. R. Stamenkovic, B. Fowler, B. S. Mun, G. Wang, P. N. Ross, C. A. Lucas, N. M. Markovic, *Science* **2007**, *315*, 493 – 497; c) M. Luo, Y. Sun, X. Zhang, Y. Qin, M. Li, Y. Li, C. Li, Y. Yang, L. Wang, P. Gao, G. Lu, S. Guo, *Adv. Mater.* **2018**, *30*, 1705515.

[6] a) A. Aijaz, A. Karkamkar, Y. J. Choi, N. Tsumori, E. Ronnebro, T. Autrey, H. Shioyama, Q. Xu, *J. Am. Chem. Soc.* **2012**, *134*, 13926 – 13929; b) J. Ying, G. Jiang, Z. P. Cano, L. Han, X. Y. Yang, Z. Chen, *Nano Energy* **2017**, *40*, 88 – 94; c) Q. Jia, S. Ghoshal, J. Li, W. Liang, G. Meng, H. Che, S. Zhang, Z. Ma, S. Mukerjee, *J. Am. Chem. Soc.* **2017**, *139*, 7893 – 7903.

[7] H. H. Wang, Z. Y. Zhou, Q. Yuan, N. Tian, S. G. Sun, *Chem. Commun.* **2011**, *47*, 3407 – 3409.

[8] a) J. de Graaf, A. J. van Dillen, K. P. D. Jong, D. C. Koningsberger, *J. Catal.* **2001**, *203*, 307 – 321; b) G. Zhao, J. He, C. Zhang, J. Zhou, X. Chen, T. Wang, *J. Phys. Chem. C* **2008**, *112*, 1028 – 1033.

[9] F. Su, F. Y. Lee, L. Lv, J. Liu, X. N. Tian, X. S. Zhao, *Adv. Funct. Mater.* **2007**, *17*, 1926 – 1931.

[10] H. Liu, D. Ma, R. A. Blackley, W. Zhou, X. Bao, *Chem. Commun.* **2008**, 2677 – 2679.

[11] J. Sun, D. Ma, H. Zhang, X. Liu, X. Han, X. Bao, G. Weinberg, N. Pfander, D. Su, *J. Am. Chem. Soc.* **2006**, *128*, 15756 – 15764.

[12] a) T. Bian, L. Shang, H. J. Yu, M. T. Perez, L. Z. Lu, C. H. Tung, Z. H. Nie, Z. Y. Tang, T. R. Zhang, *Adv. Mater.* **2014**, *26*, 5613 – 5618; b) J. Ying, J. Li, G. Jiang, Z. P. Cano, Z. Ma, C. Zhong, D. Su, Z. Chen, *Appl. Catal. B* **2018**, *225*, 496 – 503; c) J. Ying, C. Janiak, Y. X. Xiao, H. Wei, X. Y. Yang, B. L. Su, *Chem. Asian J.* **2018**, *13*, 31 – 34.

[13] P. Lu, B. Qiao, N. Lu, D. C. Hyun, J. Wang, M. J. Kim, J. Liu, Y. Xia, *Adv. Funct. Mater.* **2015**, *25*, 4153 – 4162.

[14] a) J. Ying, Z. Y. Hu, X. Y. Yang, H. Wei, Y. X. Xiao, C. Janiak, S. C. Mu, G. Tian, M. Pan, G. V. Tendeloo, B. L. Su, *Chem. Commun.* **2016**, *52*, 8219 – 8222; b) J. Ying, X. Y. Yang, Z. Y. Hu, S. C. Mu, C. Janiak, W. Geng, M. Pan, X. Ke, G. V. Tendeloo, B. L. Su, *Nano Energy* **2014**, *8*, 214 – 222.

[15] L. Feng, S. H. Li, Y. S. Li, H. J. Li, L. J. Zhang, J. Zhai, Y. L. Song, B. Q. Liu, L. Jiang, D. B. Zhu, *Adv. Mater.* **2002**, *14*, 1857 – 1860.

[16] a) J. K. Shon, S. S. Kong, J. M. Kim, C. H. Ko, M. Jin, Y. Y. Lee, S. H. Hwang, J. A. Yoon, J. N. Kim, *Chem. Commun.* **2009**, 650 – 652; b) C. M. Parlett, M. A. Isaacs, S. K. Beaumont, L. M. Bingham, N. S. Hondow, K. Wilson, A. F. Lee, *Nat. Mater.* **2016**, *15*, 178 – 182.

[17] G. Fu, K. Wu, J. Lin, Y. Tang, Y. Chen, Y. Zhou, T. Lu, *J. Phys. Chem. C* **2013**, *117*, 9826 – 9834.

[18] D. He, Y. Jiang, H. Lv, M. Pan, S. Mu, *Appl. Catal. B* **2013**, *132*, 379 – 388.

[19] M. Brun, A. Berthet, J. C. Bertolini, *J. Electron. Spectrosc.* **1999**, *104*, 55 – 60.

[20] H. S. Kim, S. Lee, D. K. Kim, Y.-W. Lee, W. C. Yoo, *RSC Adv.* **2017**, *7*, 47251 – 47260.

[21] B. Lim, M. Jiang, P. H. Camargo, E. C. Cho, J. Tao, X. Lu, Y. Zhu, Y. Xia, *Science* **2009**, *324*, 1302 – 1305.

Manuscript received: February 2, 2018
Revised manuscript received: March 18, 2018
Version of record online: April 14, 2018